recycling

MDPI

Article

Reclaiming Gold from Integrated Circuits Waste via a Sustainable Physic-Hydrometallurgical Approach

Márcia A. D. Silva [1,2], Liliana M. Martelo [1], Belmira Neto [2,3], Margarida M. S. M. Bastos [2] and Helena M. V. M. Soares [1,*]

[1] Helena M.V.M. Soares, REQUIMTE/LAQV (Laboratory of Chemistry for Life and Health Sciences), Department of Chemical and Biological Engineering, Faculty of Engineering, University of Porto, Rua Dr. Roberto Frias, 4200-465 Porto, Portugal
[2] LEPABE, ALiCE (Associate Laboratory for Innovation in Chemical Engineering), Faculty of Engineering, University of Porto, Rua Dr. Roberto Frias, 4200-465 Porto, Portugal
[3] Department of Mechanical Engineering, Faculty of Engineering, University of Porto, Rua Dr. Roberto Frias, 4200-465 Porto, Portugal
* Correspondence: hsoares@fe.up.pt; Tel.: +351-225081650; Fax: +351-225081449

Abstract

Integrated circuits (ICs), a major fraction of waste electrical and electronic equipment (WEEE), represent an important secondary source of gold (Au). However, recovering high-purity Au from ICs remains challenging due to the high silicon dioxide content that encapsulates Au within the IC core and the presence of complex base-metal mixtures that hinder selective purification. This study proposes a simplified end-to-end process that integrates mechanical liberation, magnetic separation, oxidative chlorination, ion-exchange purification and Au recovery from isolated ICs. Unlike conventional multi-stage comminution routes, the proposed pretreatment combines hydraulic pressing, milling/sieving and magnetic separation to maximize Au exposure while minimizing dust generation, metal losses and base-metal interference, which is subsequently subjected to oxidative leaching and purification. Optimal extraction conditions, determined through a Taguchi design (2.5 M HCl, 0.34 M NaClO, 40 °C, solid–liquid ratio 1 g/40 mL, 3 h), achieved a Au leaching efficiency of 89%. The resulting multi-metal leachate was treated with a strong anionic ion-exchange resin, increasing Au purity from 8% to 86% after thiourea elution in a sulfuric-acid medium. Final Au recovery was completed by reductive precipitation with sodium borohydride, yielding complete solidification (~100% efficiency). A comparative life-cycle assessment showed that this recycling route offers favourable environmental performance relative to primary mining. Beyond achieving efficient Au recovery, this work establishes an integrated recovery route for isolated ICs that combines process simplification with environmental positive impact, addressing an important gap in WEEE recycling.

Keywords: integrated circuits recycling; gold recovery; ion-exchange resin; sustainable process; life-cycle assessment

Academic Editor: Francesco Ferella

Received: 15 June 2026
Revised: 14 July 2026
Accepted: 16 July 2026
Published: 18 July 2026

1. Introduction

The growing global demand for technology has led to a significant rise in the generation of waste electrical and electronic equipment (WEEE). The Global E-Waste Monitor 2024 predicts that WEEE generation to reach 82 Mt by 2030 [1]. This WEEE is a valuable source for many raw materials, such as metals, plastic, and glass, and cannot be regarded

simply as waste without any value. Gold (Au) stands out as a critical and finite and high-value resource essential to technological advancement [2]. For this reason, new recovery strategies from secondary resources, such as WEEE, are needed to promote a sustainable solution to recover Au. Furthermore, recovering Au from WEEE is highly profitable since its concentration surpasses that found in mineral ores, around 280 $g.t^{-1}$ and 3–30 $g.t^{-1}$, respectively [3]; namely, using more environmental-friendly process than in mineral ores.

Integrated circuits (ICs), commonly known as chips or microchips, are core components in electronic devices, such as smartphones, computers, televisions, and others [4]. IC are rich in Au and composed mainly of silica (SiO_2, 62 wt.%) reinforced with brominated epoxy resin (BER) (14 wt.%) forming a solid protective structure. This matrix contains copper (Cu) (22 wt.%), iron (Fe) (1 wt.%), Au (0.3 wt.%) and silver (Ag) (0.7 wt.%), as shown in Figure 1 [5,6]. The robust physical and chemical resistance of this encapsulation presents a significant challenge for metal recovery, demanding effective pretreatment strategies.

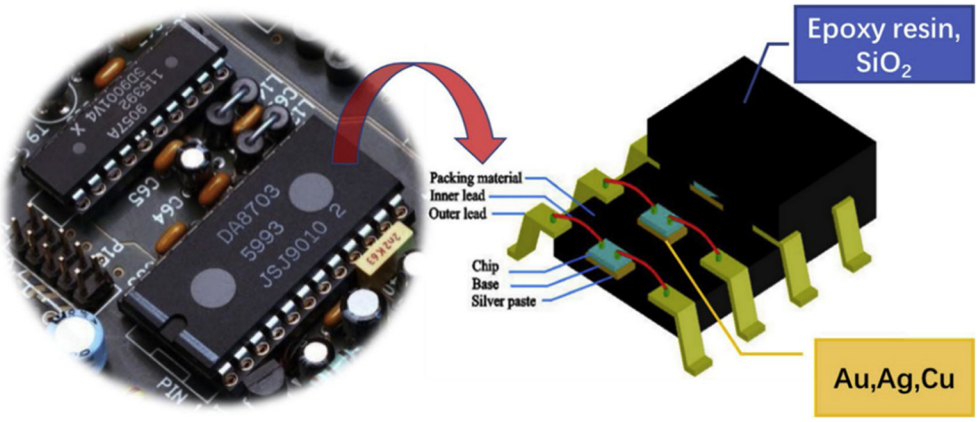

Figure 1. Schematic representation of the structure of IC and its major constituents (reprinted with permission from [5]).

Traditional approaches for treating WEEE involve thermal (e.g., pyrolysis), chemical (e.g., supercritical fluids), and physical methods [7,8]. Although vacuum pyrolysis can degrade up to 80% of organic material and enrich metal residues [9], it is highly energy-intensive and generates secondary waste products [10]. Similarly, supercritical decomposition achieves high breakdown rates of BER (95.5%) but at extreme conditions (500 °C, 23 MPa) [5]. Physical pretreatment process flowsheets are complex as they involve several steps, such as crushing, grinding, and screening to enrich the metal content for further recovery [6,11] leading to the loss of the metallic fraction throughout the sequence. In some cases, a roasting step at high temperatures (850 °C) is also added, which is not an environmental-friendly practice due to the high energy consumption and the formation of dioxins [6,11]. However, none of these processes achieve a good balance between environmental or economic impacts and efficient Au recovery because of the high energy consumption associated with a multi-step pretreatment sequence.

Considering all the limitations mentioned above, the present study proposes a simplified pretreatment process for recovering Au from IC. Furthermore, by relying solely on the intrinsic properties of the metals, it enables the separation of a magnetic fraction with a high concentration of Fe and Ni, which minimizes the interference of base metals in the subsequent Au leaching step.

Regarding Au recovery from WEEE, it is typically achieved through pyrometallurgical or hydrometallurgical techniques [9,12–14]. The recovery of Au via hydrometallurgical approaches is generally preferred due to lower energy demands and harmful emissions. Studies directly focused on IC are rarely reported in the literature and include cyanide [15]

and ionic-liquids (ILs) [16]-based processes. However, the high toxicity of cyanide and the high viscosity and costs of production of ILs associated with their difficulty of recycling and low chemical stability prevent the use of both leaching agents in Au extractive industrial metallurgy at large scale [17]. Other studies reclaiming Au from IC bearing electronic waste (such as RAM memories) described in the literature employed other leaching agents, such as halide, thiourea and thiosulfate [13,18,19]. Thiourea and thiosulfate, while less toxic, suffer from rapid oxidation in the presence of Fe(III) and Cu(II), limiting their scalability due to the massive reagent consumption as a consequence of their fast oxidation. Considering this drawback, chlorination emerges as a viable alternative for leaching Au from IC in the presence of a strong oxidant and will be evaluated in this study.

Following leaching, Au must be purified from the resulting multi-metal solution. Solvent extraction (SX) has shown limited effectiveness and cost-efficiency for low-concentration Au leachates [20,21]. For example, Doidge studied three types of amides to recover Au from a multi-metal WEEE's leachate achieving an inefficient Au extraction (less than 3%) [22]. Ion-exchange technology (IET), particularly with anionic strong basic resins, has emerged as a promising alternative for selective precious metals recovery from dilute solutions [23,24] and will be used in this work.

The development of new processes, or combinations of some, inherently entails environmental impacts. Within a sustainability framework, it is essential to ensure synergy between technological development and the assessment of the associated environmental impacts. One of the key gaps in this research topic is the lack of life-cycle assessments (LCA), particularly in comparison with primary metal extraction routes.

To date, the literature has primarily focused on identifying equipment with advantages for collection and subsequent recycling, as well as comparing different recycling pathways—namely pyrometallurgical, hydrometallurgical, and hybrid routes—for metal recovery [25,26]. These studies have also aimed to identify critical stages (such as acidic leaching, energy consumption, and mechanical pretreatment) and to guide the design of more circular processes and electronic products, including design-for-recycling strategies targeting the recovery of high-value Au [25–27]. More recently, Francini et al., studied the environmental impacts of noble metal recovery from RAM modules [28]; there is still a lack of dedicated LCA studies specifically focused on the processing of isolated ICs, which require distinct mechanical and chemical treatments.

The aim of this work is to develop an integrated and streamlined process combining physical steps with a hydrometallurgical process to recover Au at high purity from IC. The physical pretreatment includes hydraulic pressing to fragment the IC samples while minimizing dust generation followed by a simultaneous milling and sieving, and, finally, a magnetic separation to obtain a non-magnetic fraction to be used subsequently for reclaiming Au. This is followed by a hydrometallurgical process, where Au is: firstly, leached using hydrochloric acid (HCl) under oxidizing conditions; subsequently, purified through IET using an anionic basic exchange resin; and finally recovered as solid product. An environmental assessment was also conducted to evaluate the environmental impact of the complete recovery route in comparison with primary mining processes.

2. Results and Discussion

2.1. Physical Pretreatment

To recover the Au contained in the IC, the first challenge is to expose the core where the metals are located (as shown in Figure 1). To achieve this, a simplified pretreatment process consisting of three steps was developed, as shown in Figure 2.

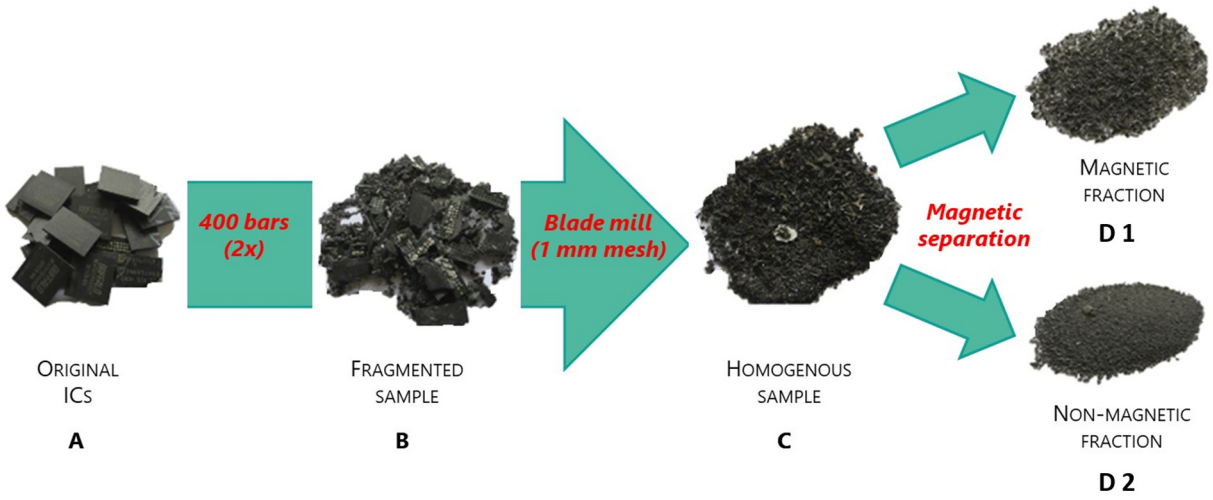

Figure 2. Scheme of the physical pretreatment implemented: (**A**) Original IC samples. (**B**) Samples fragmented after applying twice a pressure of 400 bar. (**C**) Homogenous sample after using a blade mill of 1 mm mesh, and (**D**) fractions obtained after magnetic separation, a magnetic (40 wt.%) and a non-magnetic (60 wt.%) fraction.

The developed pretreatment begins with the fragmentation of the waste IC using controlled pressure (Figure 2A) to break the main structure. Various pressures ranging from 100 to 400 bar were tested, as shown in Figure S1 (in the Supplementary Material). Based on visual analysis, the optimized experimental conditions for exposing Au were identified as applying 400 bar twice to the samples (Figure 2B). This approach resulted in a high exposure of the IC metallic fraction, which is crucial for the subsequent Au recovery. Under these optimized conditions, only 5 wt.% of dust was generated, representing minimal material loss reducing the risk of losing precious metals, as previously reported [29–31].

Although the fragmentation process (Figure 2B) effectively exposed the metallic fraction (Figure S2D in the Supplementary Material), the resulting fragments exhibited a heterogeneous particle size distribution. To overcome this, the samples were processed in a blade mill with a 1 mm mesh to homogenize their size, as shown in Figure 2C. This step does not replace the previous one, as the blades would not be as efficient without the initial fragmentation phase. Furthermore, due to the highly resistant structure of the IC, the use of only blade milling step would consume a high amount of energy and generate a higher amount of dust and, consequently, loss of metals, which would take longer to obtain a homogenous sample. On the other hand, the combination of these two steps is more universal to all types of IC, ranging from the thicker and longer ones to the smaller and thinner ones, thereby reinforcing the reproducibility of the process.

Table 1 presents the metallic composition of the IC after pretreatment. Initial sample of IC is mainly constituted by Cu (around 42 wt.%), Fe (30 wt.%), Ni and Sn (17 and 5 wt.%, respectively); all these four elements represent around 94% of the total metallic content of the sample. The remaining metal fraction contains multiple metals, such as Al, Ag, Au, chromium (Cr) and Zn, being Au-present at minor amount (0.9 wt.%) in the IC sample.

Literature describes similar composition profile of IC for the main metals (Cu, Fe and Ni) [32].

The metallic composition of the IC determined in this study should be interpreted with caution as it can vary significantly depending on the type of IC, manufacture, brand and age. Indeed Lee [6] conducted a detailed analysis of twenty-two different types of IC, highlighting substantial differences in the metallic content across various IC types. When comparing the results obtained in this study with those reported by Lee [6], the concentrations of all metallic elements were found to be in good agreement.

Table 1. Metallic composition of the samples obtained after the fragmentation procedure (IC; Figure 2C) and after the magnetic separation (Figure 2D) determined by ICP-OES after aqua regia digestion, expressed in milligram per gram (mg/g) of each sample and weight metallic percentage (% wt.) of each metal relatively to the total amount of metals present in the sample. The data represent the mean values of at least two independent experiments, performed in triplicate ($n \geq 6$).

	IC		Magnetic Fraction		Non-Magnetic Fraction	
	mg/g	**%wt.**	**mg/g**	**%wt.**	**mg/g**	**%wt.**
Cu	84.3 ± 57.3	42.3	4.3 ± 0.2	4.3	80.0 ± 11.2	81.1
Fe	59.6 ± 16.9	29.9	57.8 ± 6.5	57.4	1.8 ± 0.2	1.8
Ni	34.0 ± 1.7	17.1	30.6 ± 6.5	30.4	3.4 ± 1.5	3.4
Sn	10.3 ± 0.9	5.2	4.6 ± 1.2	4.6	5.6 ± 2.0	5.7
Pb	4.7 ± 0.2	2.4	1.3 ± 0.1	1.3	3.4 ± 1.1	3.5
Al	3.6 ± 0.8	1.8	1.2 ± 0.9	1.2	2.4 ± 0.1	2.4
Ag	0.16 ± 0.1	0.1	0.06 ± 0.01	0.1	0.1 ± 0.1	0.1
Au	1.8 ± 0.3	0.9	0.4 ± 0.05	0.4	1.5 ± 0.7	1.5
Zn	0.5 ± 0.05	0.2	0.1 ± 0.02	0.1	0.4 ± 0.1	0.4
Cr	0.1 ± 0.1	0.1	0.4 ± 0.1	0.4	0.1 ± 0.03	0.1

Given that the metallic fraction of the IC mixture contains a significant proportion of Fe and Ni (about 47.0% relatively to the total content of metals present in the sample) (Table 1), which exhibit magnetic properties, a pretreatment step included a magnetic separation. This separation process resulted in two distinct fractions of similar proportions: 40 wt.% magnetic and 60 wt.% non-magnetic (Figure 2), with distinct compositions, as shown in Table 1.

The analysis of the metallic composition of both fractions shows that the magnetic fraction is mainly constituted by Fe (about 57 wt.%) and Ni (about 30 wt.%), whereas in the non-magnetic fraction, Fe and Ni are found in minor amounts (around 1.8 and 3.4 wt.%, respectively), which demonstrates a highly efficient Fe and Ni separation from Au. Similar results were described by Barnwal and Dhawan [33]. In their work, the separation of ferrous materials (Fe and Ni) from an enriched underflow product, achieved after water fluidization of IC, increased to 57% Fe and 27% Ni in the magnetic fraction, while in the non-magnetic fraction, Cu was enriched to 83%. However, this process does not report any recovery of Au, only focusing on the recovering of base metals (Cu, Fe, Ni) and Si. In other studies, focused on the same objective of recycling IC, a more extensive pretreatment process was applied, involving additional steps and even different types of treatments [5,6,34]. On the other hand, when focusing on the recovery of Au from mining operations, the process can become even more complex, primarily because it depends on the type of ore deposit (with higher or lower concentrations of Au) and the pretreatment processes employed are often more complicated to implement, such as roasting, high-pressure oxidation, among others [35].

To our knowledge, there is no process described in the literature that enables metal exposure from the IC and simultaneously pre-concentrates Au in a distinct IC waste fraction (0.9% of Au in the metallic fraction of the original IC versus 1.5% of Au in the metallic fraction of the non-magnetic fraction) based entirely on physical treatment (Table 1). Additionally, the magnetic fraction—rich in Fe and Ni—can be further processed (e.g., pulverized and thermally treated to remove organic fraction) and repurposed for various applications. These include the use as a substitute for primary building materials in road construction, hydraulic engineering, cement and concrete production, and the synthesis of silica-based iron catalysts [36–39].

2.2. Gold Extraction

To leach Au from the non-magnetic fraction, a strong oxidizing agent (to promote oxidation of Au to Au^{3+}), together with a complexing agent to stabilize Au in solution, is needed. As mentioned in the introduction, despite extensive research on alternative non-cyanide Au lixiviants, namely, $S_2O_3^{2-}$ and $CS(NH_2)_2$ [4,6,21], none of them constitute a true alternative to halide system [22]. Among the various halides, chloride is the most suitable leaching agent due to its high stability and fast leaching kinetics [40,41]. Although these lixiviants are more selective, their practical limitations—instability, degradation, toxicity, high reagent consumption, or cost—make them less suitable for integration with the downstream purification step used in our process. In this work, the mixture of HCl combined with NaClO was used. The kinetics of Au leaching appear to be influenced by the type of hypochlorite used. In acidic media, chlorine speciation shifts toward Cl_2/HClO equilibrium, with Cl_2 being the dominant oxidizing species under strongly acidic conditions, leading to quicker gold-leaching kinetics [42]. According to the work of Baghalha [43], calcium hypochlorite has slower gold-leaching kinetics than sodium hypochlorite.

To predict the best pH and redox (Eh) conditions to stabilize the Au-Cl complex, the Pourbaix diagram was simulated for $[Au^{3+}]$ = 72 µM and $[Cl^-]$ = 1.12 M at 25 °C (Figure S2, in Supplementary Material). Under these conditions, Pourbaix diagram predicts that above an Eh of 1.1 V vs. SHE and a pH < 4, metallic $AuCl_4^-$ complex is the predominant species and should be formed according to Equations (1) and (2):

$$NaClO\ (aq) + 2HCl\ (aq) \rightarrow NaCl\ (aq) + Cl_2(aq) + H_2O \quad (1)$$

$$2Au\ (s) + 2HCl\ (aq) + 3Cl_2(aq) \rightarrow 2\ [AuCl_4]^-(aq) + 2H^+(aq) \quad (2)$$

These conditions (Eh = 1.1 V and a pH < 4) were maintained in order to allow the formation of soluble Au (III) chloro-complexes ($[AuCl_4]^-$).

Various experimental parameters, such as, NaClO and HCl concentrations, S/L ratio, time of reaction, and temperature may influence the efficiency of Au leaching rate from the non-magnetic fraction. Previous works [44,45] demonstrated that under optimized conditions (3.5 M HCl with 0.46 M of NaClO at a S/L ratio of 1/40 combined with a temperature of 40 °C during 3 h of reaction time), nearly complete extraction of Au (95 wt.%) from printed circuit boards was achieved. Based on these achievements, in this work, a DoE was performed where concentration of HCl and NaClO and S/L ratio were the main variables tested using fixed temperature (40 °C) and time (3 h). Table 2 summarizes the results obtained under each experimental condition.

Table 2. Influence of the concentration of HCl, NaClO, and S/L ratio in the efficiency of Au extraction determined by the Taguchi DoE method at a fixed temperature (40 °C), time (3 h) and agitation (150 rpm). The data represent the mean values of at least three independent experiments ($n \geq 3$); mean and standard deviations (SD) are reported as percentage of Au leached.

Run	[HCl] (M)	[NaClO] (%)	S/L (g/mL)	Au Leached (%)	S/N
1	1.5	0.27	1/10	18 ± 6	22.86
2	1.5	0.34	1/20	23 ± 3	26.95
3	1.5	0.47	1/40	58 ± 14	35.50
4	2.5	0.27	1/20	22 ± 3	26.51
5	2.5	0.34	1/40	88.6 ± 0.3	40.23
6	2.5	0.47	1/10	13 ± 2	21.65
7	3.5	0.27	1/40	79 ± 5	37.87
8	3.5	0.34	1/20	50 ± 9	33.21
9	3.5	0.47	1/10	25 ± 6	27.18

A clear trend emerges, indicating that the concentration of both reagents influences the Au leaching efficiency. At a fixed S/L ratio and NaClO concentration, increasing the HCl concentration enhances Au leaching, suggesting that higher proton availability promotes the oxidative leaching of Au. For example, increasing HCl concentration from 1.5 to 3.5 M under comparable oxidant levels and S/L ratio (Runs 2 and 8) increases the Au recovery from 23% (Run 2) to 50% (Run 8). The effect of NaClO concentration is more complex. All concentrations tested produced Eh values above the threshold required for reaction (1.1 V vs. SHE); yet the leaching response was not proportional to oxidant dosage. Moderate oxidant levels (0.34 M NaClO) improved Au leaching, whereas further increases (0.47 M) did not yield additional benefits and, in some cases, even reduced Au leaching (e.g., Run 9). A similar trend is observed at lower NaClO concentrations. This behaviour further supports that Au leaching is not governed by the nominal oxidant concentration, but rather by the effective availability of active chlorine species in solution. Under strongly acidic conditions, NaClO is rapidly converted into Cl_2, which acts as the primary oxidizing agent for Au dissolution. However, at higher oxidant level, the effective concentration of active chlorine may not increase proportionally due to volatilization of Cl_2 and non-productive side reactions, which limit its availability for Au oxidation.

Among the variables studied, the S/L ratio exhibits the strongest influence on the leaching performance. Lower S/L ratios (1/40) result in markedly higher extraction yields, as evidenced by all Runs (3, 5 and 7) where a S/L = 1/40 was used. Conversely, higher S/L ratios (1/10) were associated with lower Au extraction efficiencies (Run 9, 25% Au leached). These results suggest that decreasing the S/L ratio favours Au leaching.

Overall, the results indicate that the optimal conditions for Au leaching within the tested range are 2.5 M HCl, 0.34 M NaClO and a low S/L ratio (1/40). These parameters yield the highest Au leaching efficiency and ensure greater process stability. The S/N ratio corroborates this conclusion with the maximum value observed (40.23).

The analysis of ANOVA based on the individual replicates shows that all three factors have statistically significant effects on Au extraction ($p < 0.001$). Among them, S/L ratio is the dominant factor, accounting for approximately 78% of the total variability. HCl and NaClO exhibit secondary but statistically significant contributions (7 and 6%, respectively), reflecting their roles in maintaining the oxidative environment required for dissolution. The residual variability remains low (~8%), indicating good experimental reproducibility. The full ANOVA table is provided in the Supplementary Material (Table S1).

Considering the results obtained under optimized conditions, additional experiments were conducted to investigate the influence of the reaction time (Figure 3A) and temperature (Figure 3B). From Figure 3A, it can be observed that Au extraction reaches a high level of dissolution at the very beginning of the reaction. However, the maximum extraction is achieved after three hours, at which point the efficiency plateaus. Notably, the lowest standard deviation is also recorded at the three-hour mark. Since adsorption of Au–chloro complexes onto quartz minerals are known to occur [46] and the non-magnetic fraction used in this study consists predominantly of silica (approximately, 96% of SiO_2, determined by XRF), the leaching time was not extended further. This decision aimed to minimize the contact time between Au–Cl complexes and silica, thereby avoiding potential losses of soluble Au by adsorption. Concerning the effect of temperature, Figure 3B evidences that Au leaching increases up to 40 °C. For higher temperatures, a decrease in the Au leaching occurs due to the formation of high amount of Cl_2 gas (Equation (3)) that results in a faster consumption of NaClO (Equation (1)) [45,47].

$$HClO\ (aq) + H^+(aq) + e^- \longleftrightarrow \frac{1}{2}Cl_2(g) + H_2O(l)\ E^+/V = 1.611 \quad (3)$$

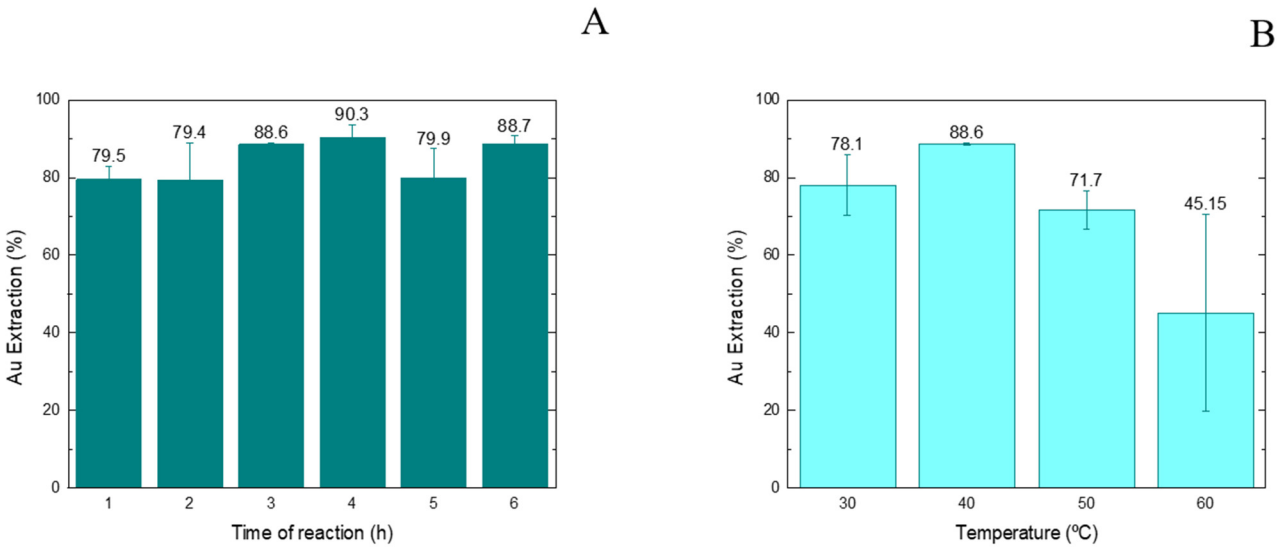

Figure 3. Influence of the time of reaction ((**A**), with fixed 40 °C) and temperature ((**B**), with 3 h fixed). The experimental conditions were fixed at concentration at HCl (2.5 M), and NaClO (0.34 M), and S/L ratio (1/40). The data represent the mean values of triplicates; standard deviations (SDs) are presented (vertical error bars). Where no error bars are shown, SDs are within the points.

From these results, the following optimal experimental conditions for Au extraction were defined: 2.5 M HCl and 0.34 M NaClO, with an S/L ratio of 1/40, at 40 °C for 3 h. These conditions allowed achieving a high Au leaching yield (89%) from the non-magnetic fraction residue.

Beyond its influence on leaching kinetics, the formation of Cl_2 at elevated temperatures also introduces important operational and environmental considerations. HCl/HClO systems offer clear advantages—fast dissolution kinetics, high stability of Au–Cl complexes, and the ability to operate under relatively mild conditions. However, an inherent drawback is the potential generation of Cl_2, particularly under strongly acidic and high temperature regimes. This gas is corrosive and hazardous, requiring strict containment and gas-handling measures. In the present work, operating at 40 °C and using optimized oxidant concentrations effectively mitigates Cl_2 evolution, ensuring high Au extraction while minimizing volatilization losses and safety risks. Moreover, several metal alloys can be used to prevent corrosion problems from this type of system [48]. The neutralization of chlorine gas formed can be neutralized, for example by metal–organic framework (MOF) [49].

There is a real concern that Au dissolution and Au cementation can occur at the same time when residual Cu and Al remain present in the IC leaching, which lowers apparent Au recovery and makes selective process control harder [50]. In order to minimize these effects, immediately after leaching the remained solid was removed by filtration.

At the end of this process, we obtained a non-magnetic fraction with a high Si content, which can be used in the production of glass and ceramics, as well as in the applications already mentioned for the magnetic fraction [36–39].

The obtained results compare favourably with literature for chloride-based Au leaching systems. Bui [51] achieved nearly complete Au extraction from waste-printed circuit boards using a chlorate/HCl system operated at 55 °C for 5 h. Baghalha reported a maximum Au extraction of 67% from a silica-rich ore under optimized HCl/NaClO conditions. Similarly, Filcenco [52] obtained 98% Au extraction from a Cu–Au slag using higher HCl concentration (4 M) and longer reaction times. In refractory Au ores, Fu [53] reported a maximum Au extraction of 68.6% using a NaClO concentration approximately four times higher than that employed in the present study. Likewise, Hasab [47] reported that three

successive chloride–hypochlorite leaching stages were required to achieve 96% Au extraction from a refractory pyritic concentrate. These conditions contrast with the developed process in this work, which achieves high extraction efficiency in a single step and under significantly milder operational conditions. Although direct comparisons should be made with caution due to differences in feed composition and mineralogy, the results obtained in this work demonstrate that high Au extraction efficiencies can be achieved under relatively mild operating conditions using a simple single-stage chloride–hypochlorite leaching process. Overall, this study shows that high Au extraction efficiencies can be achieved without resorting to elevated temperatures, multi-stage leaching or excessive oxidant concentrations, reinforcing the relevance and competitiveness of the process developed.

2.3. Gold Purification

As it is shown in Figure 4, the leachate obtained under the optimized conditions corresponds to a multi-metal solution mainly constituted by Cu, Ni, Sn and several other metals (Ag, Al, Cr, Cu, Fe, Ni, Pb, Sn and Zn) besides Au, which is present at low grade (<8 wt.% in the leachate solution), and, thus, needs a purification step.

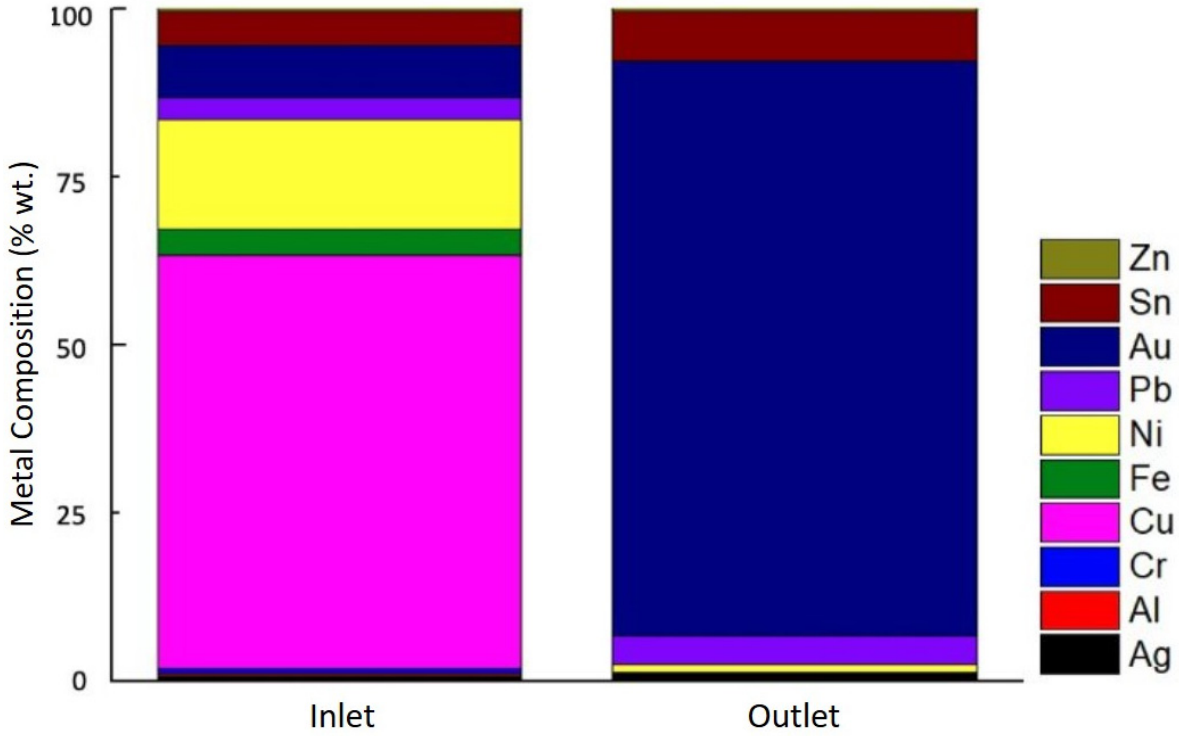

Figure 4. Metallic composition (wt.%) of the leached solution obtained under optimized conditions and the final eluate solution after adsorption with Purogold^{TM} A194 resin and elution process.

Under the Eh-pH conditions of the leachate, Pourbaix diagram (Figure S2, in the Supplementary Material) points out that $AuCl_4^-$ is the predominant species of Au. Strong anionic exchange resins have been recognized as effective for recovering Au from acid chloride leach solutions [45,54] through an ion-exchange interaction mechanism, as exemplified by Equation (4):

$$\vdash N^+R_nX^- + [AuCl_4]^- \Longleftrightarrow \vdash N^+[R_nAuCl_4]^- + X^- \quad (4)$$

where the symbol $\vdash$ denotes the inert matrix (polymer structure) of the resins and n takes values between 1 and 3 according to the resin. When $n < 3$, R is replaced by hydrogen atoms (the number of hydrogen atoms is equal to $3 - n$).

Therefore, in this work, Purogold™ A194 resin, which is a strong anionic exchange resin, was selected to evaluate its potential for separating and concentrating Au from the multi-metal leachate solution following the rational for its higher total exchange adsorption capacity (1.98 eq/L) [55] comparatively to others resins, such as MTA 5011 (1.15 eq/L) and Amberjet 4200 (1.3 eq/L) [56]. For this purpose, continuous column mode assays to purify Au from the multi-metal-leached solution were performed. After preliminary optimization of the experimental parameters (bed volumes and flow), Figure 5 presents the various breakthrough curve profiles for the various metals, which lasted up to 26 h when 10% of Au was present in the raffinate solution.

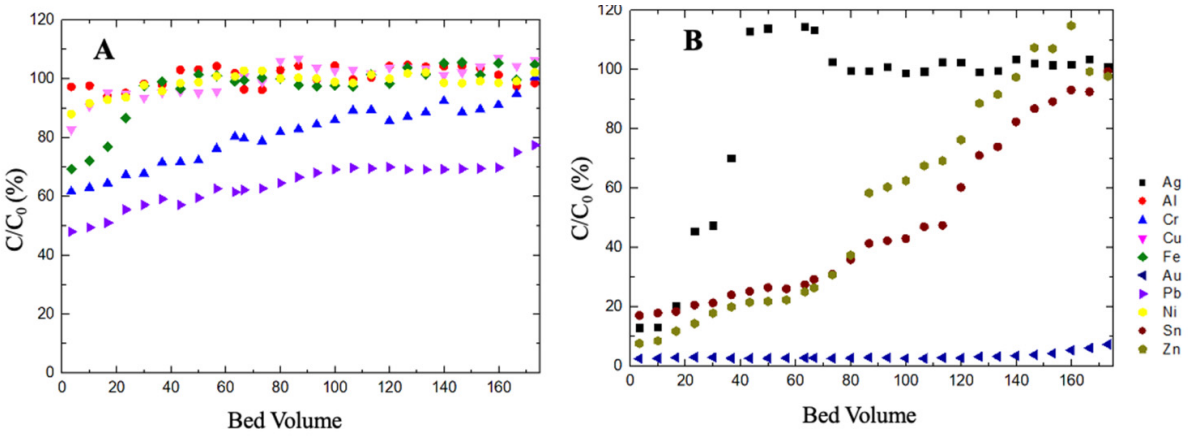

Figure 5. Graphical representation of the ratio between the metal concentrations in the outlet, C, and in the inlet solution, C_0, versus bed volumes (around 2 mL) for a real leachate solution where in (**A**) metals exhibited negligible adsorption by the resin, maintaining C/C_0 values close to 100% across the tested bed volumes. (**B**) Metals showing significant affinity for the resin, with C/C_0 decreasing markedly at low bed volumes due to effective retention during column operation. Flow rate of 0.225 mL/min was used.

As can be seen from Figure 5, Au evidenced the highest affinity for the resin being totally adsorbed until the breakthrough point was observed after 174 BV (Figure 5B) whereas Al, Fe, Ni and Cu did not show any significant affinity for the resin (Figure 5A). In addition, Fe, which has shown a slight adsorption to the resin in the beginning (up to 40 BV), all other metals evidenced a complete breakthrough (C/C_0 = 100%) since the beginning of the experiment. Other metals, such as, Ag, Zn and Sn (in that order), evidenced affinity for the resin but considerably lower than Au (Figure 5B). In the case of Ag, a fast and complete breakthrough was observed within the first 6.5 h (60 BV) whereas, for Zn, C/C_0 increased gradually up to 80 BV, after which, C/C_0 jumped reaching values > 100% after 140 BV. These results show that all adsorption spaces occupied by the negative chloride species of these two metals (Ag and Zn) were exchanged by $AuCl_4^-$ species until the breakthrough for Au was achieved. Therefore, Al, Ag, Fe, Ni, Cu and Zn are not expected to be present in the eluate. In the case of Sn, C/C_0 increased gradually up to 110 BV, after which, C/C_0 jumped up to 100% after 180 BV, exactly when 10% of Au was present in the raffinate solution (26 h). Finally, Pb and Cr evidenced affinity for the resin but less comparatively to Zn, Sn and above all Au (Figure 5A).

These results suggest that, under the experimental conditions used, Purogold™ A194 resin presents the following metal affinity order: Au >> Sn > Pb > Zn > Cr > Ag >> Fe > Cu ≈ Ni ≈ Al. These metal adsorption profiles can be explained by the metal chemical species present in solution. In fact, computer chemical speciation simulations predict that, under the experimental conditions used, besides Au, which is totally present as $AuCl_4^-$ species, Ag, Sn, Pb and Zn are also mainly present as negative chloro-complexes [Ag, as $AgCl_x^{-(x-1)}$,

Sn as $SnCl_5^-/SnCl_6^{2-}$ species and Pb or Zn, mostly (≥95.3%) as MCl_3^-/MCl_4^{-2} species)], which are adsorbed by the anionic resin through an ion-exchange interaction mechanism.

Additionally, a raffinate solution remained after the adsorption step. This solution contains various metals [majorly, Cu (69 wt.%), Ni (18 wt.%), Fe (4 wt.%), Sn (3 wt.%) and Pb (2 wt.%)] at low levels, which should be treated by precipitation process to achieve the discharge requirements established in the Urban Wastewater Treatment Directive (EU Directive 91/271/EEC, revised by Directive (EU) 2024/3019) [57]. Precipitated can be seen as a co-product because it can be redissolved and precipitated separately or in alloy shape [58].

The approximate Au dynamic uptake capacity of the resin (Q_0, expressed as mg Au/g of the resin) was calculated using Equation (5).

$$Q_0 = (C_0 - C_t) \times V/m \quad (5)$$

where Q_0 is the amount of Au adsorbed (in mg/g of resin), C_0 and C_t are the concentration of Au in the inlet solution and in the outlet at a given time or volume (mg/L), respectively, V is the volume of solution that has passed through the column (L) and m is the mass of resin used (g).

An Au dynamic uptake capacity value of 31.3 mg/g was achieved for Purogold™ A194 resin and is presented in Table 3 together with values for other resins. Table 3 shows that the value obtained in this work (31.3 mg/g) is the second highest, only surpassed by the value for Puromet MTS9140 resin (42 mg/g). Table 3 also shows a wide range of Q_0 values (about one decade) for the various resins. Nevertheless, the Q_0 values should be analyzed with care since the capacity of each resin to adsorb Au ions is affected by several factors, such as the nature of the resin, nature, and concentration of the competing ions present in the matrix solution. In fact, Table 3 shows a much lower Q_0 value for Purolite A200 (4.7 mg/g) relative to Purogold A194 resin (31.3. mg/g), that are both anionic resins, which may be explained by the highest affinity of thiosulfate and TU present in the matrix solution for Au. These results point out that the optimization of both leaching and purification steps should be designed together to promote synergistic effects aiming the highest yield and purity.

Table 3. Comparison of the Au dynamic uptake capacity value for various resins and the resin used in this work (Purogold™ A194).

Resin	Nature of Resin	Matrix Solution (M)	Au (q_0) (mg/g)	Reference
Purolite® A200	Type II quaternary ammonium	1.71×10^{-4} of thiosulfate and 0.13 of TU	4.7 ± 0.3	[59]
Lewatit® MonoPlus TP 214	Chelating (TU)		13 ± 1	
Dowex™ M-4195	Chelating (bispicolylamine)		25 ± 6	
Puromet® MTS9140 (thiourea)	Chelating (TU)		42 ± 7	
Purogold™ A194	Strong anionic	2.5 of HCl and 0.34 of NaClO	31.3 ± 3.2	In this work

The elution of Au adsorbed to Purogold™ A194 resin was promoted using a solution containing TU and sulfuric acid (0.25 M CH_4N_2S and 0.5 M H_2SO_4, respectively) for 2 h with a flow rate of 0.50 mL/min. During this desorption stage, Au(III) is reduced to Au(I)

and then complexed with TU [60] which is released to the bulk solution, according to Equation (6):

$$\vdash N^{+}[R_nAuCl_4]^{-} + 2\,TU \Longleftrightarrow \vdash N^{+}R_nCl^{-} + [Au(TU)_2]^{+}Cl^{-} + Cl_2 \quad (6)$$

After 1h, 76% of the adsorbed Au was eluted resulting in an eluate solution containing 741 mg/L of Au, and after 2 h, 91% of the adsorbed Au was eluted bringing the concentration of Au down to 444 mg/L. Therefore, an elution time of 120 min was defined and a final solution containing Au with high purity grade (85.3%) was achieved, where Sn was the major contaminant (7.5%) followed by Pb (4.3%). Even though Cu, Fe and Ni were present at a significant amount in the leachate (61, 4 and 16%, respectively), no significant adsorption of these metals has occurred in the PurogoldTM A194 resin (Figure 5A) since no anionic chloride species of these metals are formed under the chemical conditions used. Thus, minor amounts of Cu, Fe and Ni were detected in the eluate (0.2, 0.3 and 1.1%, respectively). On the other hand, a slight concentration of Pb and Sn in the eluate relative to the inlet solution (Figure 4) occurred due to adsorption of the anionic chloride complexes of these two metals to the resin by a similar mechanism described for Au. The competitive effect of metals that form negative chloro-complexes (such as, Ag, In, Pb and Sn) in the separation of Au and other precious metals from multi-metal solutions using anionic exchange resins has been described in the literature [45,54,61].

A final solution containing Au with a purity of 86% was achieved, being more than 10 times greater than the percentage of Au in the inlet solution (7.8% Au) with Pb and Sn as the main impurities (see Outlet Composition in Figure 4). These results correspond to a good compromise between achieving a high Au purity in the eluate and minimizing the loss of Au to the raffinate (10% of lost) (Figure 5B). Purogold™ A194 resin has proven effective in extracting Pt from a chloride leachate [62], showing that Pt can be reused across several adsorption–elution cycles (at least five cycles of adsorption–washing–elution–washing). Given that both studies utilized comparable oxidizing chloride environments, it is reasonable to believe that Purogold™ A194 resin might also be effective in recovering Au while retaining its efficiency through numerous regeneration processes.

Different $NaBH_4$ concentrations were evaluated for Au reduction, and under the optimal condition (0.5 M $NaBH_4$), Au was almost completely precipitated from solution. A preliminary analysis of the dried precipitate suggested that its composition was consistent with the eluate. This step enabled the production of a solid Au product and the assessment of the complete recovery route in the environmental analysis.

3. Environmental Impact: Developed Process vs. Primary Extraction

As described in the methodology, the boundaries of the environmental impact assessment are presented in Figure S3 in the Supplementary Material. This figure illustrates a simplified scheme of the implemented process alongside a parallel comparison with the database processes considered in the LCA study.

Figure 6 shows results for 18 impact categories across all assessed Au production methods, allowing comparison between the developed process and those used worldwide. Overall, two Au production processes stand out negatively in most of the impact categories: the Au production mining processes for Chile (Gold CL) and for Australia (Gold AU). The reasoning behind theses profiles is discussed below. Table S2 shows the absolute values obtained for the 18 ReCiPe environmental impact categories evaluated per Au production process assessed and, for the developed process, the percentage allocated to each step.

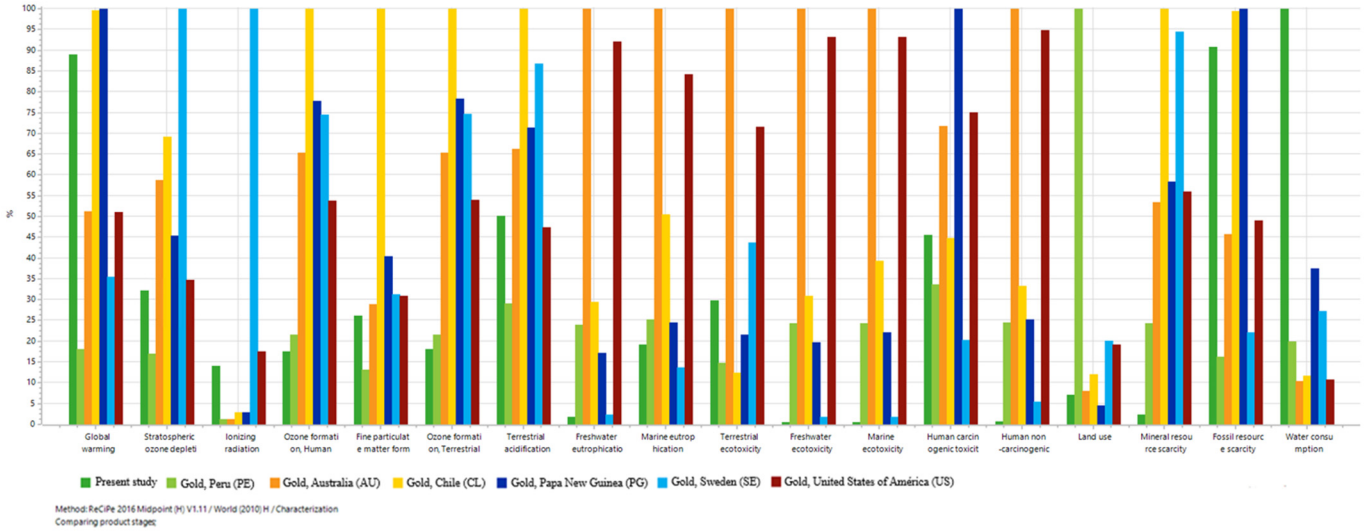

Figure 6. Environmental impact assessment results (ReCiPe 2016 Midpoint, Hierarchist perspective) from the developed process (Present study) and different Au production processes taken from Ecoinvent 3.11 database. Results are reported to the functional unit of 1 mg of recovered solid Au. The bars represent: present study (green), mining operation in Sweden (SE, blue), Au production in Australia (AU, orange), mining operation in Chile (CL, yellow), mining and refining operation in Papua New Guinea (PG, dark blue), and gold–silver ingot production in Peru (PE, light green).

The process developed in the present study shows the lowest contribution to nine impact categories. Water consumption is the only category where the impact is the highest. Renewable energy, present in the Portuguese electricity mix production, requires heavy water use associated with energy generation, especially from hydropower sources. Other categories, such as global warming and fossil resource scarcity, also stand out due to the small percentage of natural gas used in the Portuguese energy-mix production.

An in-depth analysis into the unit processes shows that, across all categories, the Au leaching step has the largest impact (as seen in Table S2). Although throughout the process 11% of Au is not recovered, the addition of a second leaching step would have an even larger impact in the LCA of the process. It is not surprising, as this step relies on chemicals which production contributes to impacts across all categories and is the step with highest energy consumption. It is worth noticing that in two categories (marine eutrophication and mineral resource scarcity) the impact of the purification step is largely associated with the production of TU and $NaBH_4$.

One example of process with larger impact is the Chilean mining process that exhibits higher impacts in seven out of the 18 assessed categories. These impacts are primarily driven by fossil CO_2 and NO_x emissions associated with an electricity mix heavily reliant on natural gas and coal. Additionally, this process stands out in terms of mineral resource scarcity (≈1% loss of Au mass) and fossil resource scarcity due to coal consumption.

The Australian mining process shows higher impacts in 6 categories, notably in freshwater and marine eutrophication, as well as ecotoxicity. These impacts are linked to phosphate and nitrate emissions, and to the release of metals (Hg, Cu, Zn) associated with the treatment of sulfidic tailings generated in open-pit mining operations.

The Swedish process is distinguished by higher impacts in stratospheric ozone depletion due to extensive use of explosives and ionizing radiation, associated with the share of nuclear energy in the electricity mix. In Peru, land use is the most impacted category, mainly due to the prevalence of open-pit mining.

These three processes have two different points that impaired its environmental impact: a non-sustainable energy mix (using nuclear energy or coal) and the formation of

secondary tailings. So, the developed process has made strong efforts and commitment toward high process efficiency and time optimization to reduce energy consumption, since it reveals to be the more important point. Although the study has its limitations due to the use of a laboratory scale, the process proves to be a promising alternative to recover Au when compared to the worldwide Au mining processes. In industry scale, the difference would be higher in a positive way. Our findings are consistent with those concluded by Francini [28] work, where it was pointed out that the leaching step is the most impactful one and recovering Au from WEEE has lower environmental impact than primary mining, even applying to Au extraction from IC-bearing components (RAM memories), even though both works have very distinct functional units and system boundaries, which strengthens both conclusions even more.

4. Materials and Methods

4.1. Materials

All chemical reagents used were of analytical grade: HCl 37% purchased from VWR Chemicals, nitric acid (HNO_3) 70% purchased from PanReac-AppliChem, sodium hypochlorite (NaClO) 13% (v/v) purchased from Supelco®, sulfuric acid (H_2SO_4) 98%, thiourea (CSN_2H_4, TU), and sodium hydroxide (NaOH) all from VWR, sodium borohydride ($NaBH_4$) from Sigma-Aldrich (St. Louis, MO, USA).

A strong anionic exchange resin with a polystyrene structure cross-linked with divinylbenzene functionalized groups of mixed tertiary amine and quaternary ammonium was used (designated as Purogold™ A194, from Purolite®, King of Prussia, PA, USA).

4.2. Methods

4.2.1. Physical Pretreatment of the IC

Ten kilograms of IC were detached from the waste of printed circuit boards (PCBs) from various personal computers and laptops, collected from local technological stores, and used throughout all the work without any selection of the type of IC.

The IC samples were then fragmented (10 g per assay) inside a closed tube of stainless steel using a hydraulic press by Meganor (Bragança, Portugal). Different pressures (ranging from 100 to 400 bar) were tested aiming for producing a higher exposition of metals and, simultaneously, minimizing the production of dust. The loss of mass, as dust, was calculated considering the difference between the mass of IC samples before and after the pretreatment process. The criterion for selecting the force to be applied was determined by the highest level of metal exposure combined with the lowest percentage of dust loss. After choosing the correct pressure, an additional step to homogenize the size and dimensions of the mixture of the fragmented IC was performed using a blade mill from Retsch 200 equipment (Retsch GmbH, Haan, Germany) (blade with 1 mm mesh, which allows the simultaneous milling and sieving of the sample in only one step).

Finally, the magnetic separation was carried out using a magnetic stirrer (VWR, Radnor, PA, USA) at 100 rotations per minute (rpm) with a strong magnet of 400 kJ/m^3 to obtain two (magnetic and non-magnetic) fractions.

4.2.2. Gold Extraction Procedure

All experiments to extract Au were performed with combination of HCl and NaClO. To study the optimum experimental conditions, an experimental design with Taguchi method was applied for maximizing the leaching efficiency of Au. Table 4 presents the three factors (concentrations of HCl, NaClO, and different solid-to-liquid ratio) and each three levels chosen. All experiments were conducted in a shaking bath with fixed temperature and agitation of 150 rpm in a thermostatic bath (OLS200, Grant, Royston, UK). The upper and

lower boundaries of the three levels were determined based on preliminary tests to ensure a detailed analysis. Each run included at least three replicates.

Table 4. Controllable factors, namely A—concentration of HCl (M); B—concentration of NaClO (M); and C—Solid/Liquid Ratio (g/mL) and their levels. Each experiment was run during three hours at 40 °C.

Factor	Description	Level 1 (L1)	Level (L2)	Level (L3)
A	[HCl] (M)	1.5	2.5	3.5
B	[NaClO] (M)	0.27	0.34	0.46
C	S/L ratio (g/mL)	1/10	1/20	1/40

The chosen statistical parameter was Signal-to-Noise (S/N) ratio to obtain a statistical assessment of the process performance. Depending on the type of analysis required, there are three types of S/N: (1) smaller is better, (2) nominal is best, and (3) larger-the-better, where the most suitable one is larger S/N because, in this case, the aim is to increase the percentage of Au extracted. The S/N ratio for the case of larger-the-better was evaluated through Equation (7).

$$\frac{S}{N} = -10\, log\left(\frac{1}{n}\sum_{i=1}^{n}\frac{1}{R_i^2}\right) \quad (7)$$

where R_i is the percentage of Au leached in replication experiment "i", which was conducted under the same experimental conditions for each test run, and "n" is the total number of replications of each test run.

The optimal process conditions can then be determined from the table by identifying the level at which a process parameter has maximum value S/N value. Furthermore, the statistical significance of the experimental factors was evaluated using analysis of variance (ANOVA). The ANOVA was performed in R (version 4.6.1) using the classical linear model applied to the individual replicate measurements. This approach allows proper estimation of the experimental error and increases the degrees of freedom of the residuals, providing statistically robust F-tests and p-values.

After obtaining optimum value for the chosen factors, the study of kinetics and temperature was performed. Each test was performed in triplicate.

To evaluate the overall metal-leaching yield, total acid metal digestion of the final solid residue remained after each leaching assay was carried out using aqua-regia (3/1 (V/V) of HCl/HNO_3) for all the samples.

The Eh–pH diagrams of dissolved Au-chloride species at 25 °C were drawn using the SPANA software (Visual basic version, Stockholm, Sweden). Chemical speciation simulations were carried out using the MINEQL+ software (5.0 version).

4.2.3. Gold Purification Procedure

For purification of Au from the multi-metal leachate solution achieved under optimized conditions, a rigorous amount of the Purogold^{TM} A194 resin, representing 0.66 bed volumes (2 mL), was transferred to the chromatographic glass column (di = 6.6 mm, h = 100 mm) with water in agreement to the manufacturer's specifications [55]. The optimized flow rate used (0.225 mL/min) was controlled using an MS-Reglo peristaltic pump (Ismatec, Glattbrugg, Switzerland). Elution was performed using a solution with 0.25 M CSN_2H_4 in 0.5 M H_2SO_4 at the same flow rate for 120 min. Between adsorption and elution, the resin was washed with 30 mL of deionized water, and after elution, the resin was washed with 60 mL of deionized water and reused again. Experiments with synthetic solutions were performed in replicate for process optimization ($n \geq 4$). Tests with real leachate were conducted for validation under realistic conditions.

The purified Au solution obtained after ion-exchange purification was subjected to a solidification step using $NaBH_4$ as a reducing agent. Different $NaBH_4$ molar concentrations (0.06, 0.09, 0.15, 0.3 and 0.5 M) were preliminarily evaluated to determine the conditions required for efficient Au precipitation. The precipitate was separated from the solution, washed, dried and quantified.

4.3. Metal(oid)s Quantification

The quantification of silica of the samples was obtained by X-ray fluorescence (WD-FRX Axiosmax 4 kW) (Malvern Panalytical, Almelo, The Netherlands) with a vial of Rhodium. The samples were first heated at 800 °C during 1 h to remove all the organic compounds (≅10 wt.% of weight loss was registered before and after the heating) and then, a semi-quantitative analysis was performed using the Omnian software from Panalytical (Malvern Panalytical, The Netherlands).

For the other elements, quantification was performed on liquid samples after aqua regia digestion, using flame atomic absorption spectroscopy (AAS-FA) in a Perkin Elmer AAnalyst 400 spectrometer (Perkin Elmer Inc., Norwalk, CT, USA) or in an Analytik Jena novAA350 spectrometer (Analytik Jena AG, Konrad-Zuse, Germany); nitrous oxide-acetylene flame was used for tin (Sn) and aluminum (Al) and air–acetylene flame was used for the remaining metal quantifications. Additionally, metal concentrations in the leaching solutions were quantified by Inductively Coupled Plasma—Optical Emission Spectrometry (ICP-OES), using an ICAP 7400 THERMO spectrometer (Thermo Fisher Scientific, Waltham, MA, USA) equipped with a nebulizing system and when metal concentration is bellow AAS-FA detection limit, using a multi-element standard solution.

When necessary, the redox potential (Eh) of the leachate was measured with a Pt indicator electrode using a Metrohm 744 pH metre (Metrohm AG, Herisau, Switzerland).

4.4. Life-Cycle Assessment

4.4.1. Goal and Scope of Study

An LCA study was performed to assess the environmental impact of the developed process and compare it with the conventional mining for Au extraction and DORÉ bar production. The LCA followed the ReCiPe 2016 midpoint (Hierarchist) method, implemented in SimaPro 10.2.0.1 using Ecoinvent 3.1. 1 Midpoint indicators were selected to reduce uncertainty and avoid value laden aggregation associated with endpoint modelling, which is particularly relevant for metallurgical systems due to the release of toxic emissions and use of chemicals [25]. The LCA study used 1 mg of Au produced as the functional unit.

4.4.2. Inventory

The detailed inventory for the process developed is presented in Table 5, regarding the inputs and outputs applied in SimaPro. All values presented were calculated to obtain 1 mg of Au at the end of the process. To allow comparison, the chosen datasets for Au extraction processes yield a partially purified product prior to the refining stage. Datasets represent diverse geographical and technological contexts across Peru, Australia, Chile, Papua New Guinea, Sweden, and the United States. The selected databases capture the global variability in mining and beneficiation. All use cyanide leaching but differ in the recovery methods. In general, the cyanide-impregnated solution undergoes carbon-in-pulp or electrowinning process to further be precipitated with zinc dust. The last step is smelting to obtain DORÉ bars. One limitation of these datasets is the lack of DORÉ purity. Only the Swedish dataset reports a purity of 79%, which is within the DORÉ ranges that typically stays between 50 and 90% Au [63]. To ensure a consistent comparison, the Au purity of the developed process (86%) is considered within the range of doré bar compositions (50–90% Au), enabling alignment between the partially refined literature datasets and the

final product of this study. All values were measured and reported to 1 mg of solid Au. Figure S3 shows a parallel scheme to better understand the limits of all datasets.

Table 5. Input and output flows considered in the LCA model of the developed process to recover 1 mg of Au. The selected ecoinvent databases from ecoinvent 3.11 related to each designation used.

		Reference Flow
Inputs	Raw material	0.87 g Integrated Circuit
	Energy	0.171 KWh eletricity, high voltage PT production mix
	Chemicals	1.82 g HCl (2.5 M) 0.51 g NaClO (0.34 M) 0.098 g TU (0.25 M) 0.057 g H_2SO_4 (0.5 M) 1.6 g NaOH (2 M) 0.056 g $NaBH_4$ (0.5 M)
Outputs	Product	1 mg of solid Au
	Emissions to water	0.023 L wastewater *
	Emissions to air **	0.049 g Silicates
	Co-products	Metals: Cu: 82.74 mg; Fe: 58.5 mg; Ni: 33.37 mg; Sn: 10.11 mg; Pb: 4.09 mg Silicon: 0.932 g
Processes		**Ecoinvent database V.3.11**
Gold, Peru (PE)		Gold-silver, Ingot {PE}| gold mine operation with extraction | Cut-off, U
Gold, Australia (AU)		Gold {AU} | gold production | Cut-off, U
Gold, Chile (CL)		Gold {CL} | silver-gold mine operation with refinery | Cut-off, U
Gold, Papa New Guinea (PG)		Gold {PG}| gold-silver mine operation with refinery | Cut-off, U
Gold, Sweden (SE)		Gold {SE}| gold mine operation and refining | Cut-off, U
Gold, United States of America (US)		Gold {US} | gold production | Cut-off, U

* Wastewater composition complies with parameters required to discharge according to Urban Wastewater Treatment Directive (EU Directive 91/271/EEC, revised by Directive (EU) 2024/3019) [57]. ** Emissions to air represents the fines lost during the pre-treatment process.(about 5% of initial sample).

The energy mix in the Ecoinvent database for each country was compared with the energy mix presented in the IEA 2023 data [64]. To reproduce the more precise dataset, the percentage contributions of each energy source were adjusted by replacing the corresponding datasets from Ecoinvent 3.11 in datasets from Peru and Chile. The other datasets remained intact because the energy mix did not change significantly.

5. Conclusions

The recovery of Au from IC remains a critical issue at the intersection of waste management and natural resource conservation. This study successfully developed and validated a fully integrated physical–hydrometallurgical route specifically tailored for Au recovery from isolated ICs. While recent literature has focused mainly on entire printed circuit boards or RAM modules, this work tackles a significant challenge in designing an efficient process lies in removing the encapsulation shell of the IC and recovering Au with high purity from the complex matrix rich in various metals of the IC. For that purpose, this work describes a methodology, based on a three-step physical process that increases the exposure of the metallic fraction for effective Au recovery and, simultaneously, minimizes the dust production and consequent loss of valuable metals. Integrating physical pretreatment with a hydrometallurgical route improves significantly the Au recovery performance from IC,

representing an innovative approach and contributing positively to the advance of the current state of the art in this field. On the opposite side, the literature so far presents pretreatment process as very complex (with large number of steps) and associated with a loss of mass during the steps.

The physical process comprises the fragmentation of the IC samples under 400 bars of pressure (twice) using a hydraulic press, homogenization of the fragmented material and a magnetic separation. This methodology originated just 5% of material loss. This approach yielded two distinct fractions: a non-magnetic fraction and a magnetic fraction composed mainly of Fe and Ni. The reduction in base-metal content in the non-magnetic fraction allowed an enrichment of Au from 0.9 to 1.5%wt, which contributed for using less quantity of leaching agent in the subsequent step. After optimization of the key parameters through DoE using Taguchi method, a leaching yield of 89% of Au was achieved at 40 °C for 3 h, using a ratio of S/L of 1/40 g/mL with 2.5 M of HCl and 0.34 M of NaClO. ANOVA analysis allowed to conclude that S/L ratio is the factor with higher impact (78%). To purify the multi-metal-leached solution (containing Ag, Al, Cr, Cu, Fe, Au, Pb, Ni, Sn, and Zn), the selective Au adsorption using a strong anionic exchange (Purogold^{TM} A194) resin was implemented and optimized. The resin evidenced high affinity for Au over other metals, achieving a Au adsorption rate above 90% while the adsorption rates for the other metals were significantly lower. A final solution containing 86% of Au, ten times more concentrated than the inlet solution, was achieved after eluting Au from the resin with TU and sulfuric acid. The purified Au solution was subsequently solidified with nearly complete recovery, allowing the production of a final Au product. The treated raffinate solution after alkalinization can be safely discharged in public water systems, demonstrating the environmental sustainability of the process. The natural variability of IC residues underscores the need for continuous monitoring of feed composition during adsorption-based purification. In industrial operation, periodic Au quantification would enable adaptive adjustment of key parameters—particularly adsorption time—supported by data-driven or AI-based control models to ensure stable performance. Further automation of IC removal from printed circuit boards would enhance process consistency and overall operational efficiency. Crucially, this work provides the first LCA specifically dedicated for recycling isolated IC. The results proved that this specialized route offers a more favourable environmental performance than primary mining across various global contexts. By demonstrating the potential for valorizing secondary fractions (magnetic and silicates) and ensuring safe wastewater discharge, this process aligns with circular economy principles. Overall, the results demonstrate that recovering Au from IC is feasible with positive environmental impact against traditional mining. This work demonstrated a futurist prospect for the recovery of Au from this stream, as well as recovering other ferrous metals, contributing to sustainable resource management and environmental protection.

Supplementary Materials: The following supporting information can be downloaded at https://www.mdpi.com/article/10.3390/recycling11070127/s1, Figure S1: System boundary diagram for the comparative LCA of two gold recovery routes; Figure S2: ICs samples obtained at the end of the fragmentation process applying; Figure S3: Pourbaix diagram for the $Au^{3+}/Cl^{-}/e^{-}$ system pH. versus E(SHE), for $[Au^{3+}]$ = 72 μM; $[Cl^{-}]$ = 1.12 M at 25 °C; Table S1: Analysis of variance (ANOVA) for Au extraction based on individual replicate measurements; Table S2: Comparative life cycle impact results for the present study and gold production datasets.

Author Contributions: M.A.D.S.: Conceptualization. Data curation. Investigation. Writing—original draft; L.M.M.: Conceptualization. Formal analysis. Methodology. Writing—original draft. Supervision. Writing—review and editing. B.N.: Supervision. Writing—review and editing. M.M.S.M.B.: Funding acquisition. Project administration. Resources. Validation. H.M.V.M.S.: Conceptualization. Writing—original draft. Funding acquisition: Project administration. Resources. Supervision. Vali-

dation. Writing—review and editing. All authors have read and agreed to the published version of the manuscript.

Funding: This work is financially supported by national funds through the FCT/MCTES (PIDDAC), under the project PTDC/CTA-AMB/3489/2021—RECY-SMARTE—Sustainable approaches for recycling discarded mobile phones, with DOI 10.54499/PTDC/CTA-AMB/3489/2021 (DOI: https://doi.org/10.54499/PTDC/CTA-AMB/3489/2021) and also through the project UID/50006/2025 DOI 10.54499/UID/50006/2025—Laboratório Associado para a Química Verde—Tecnologias e Processos Limpos. From the Laboratory for Process Engineering, Environment, Biotechnology and Energy (LEPABE), it was funded by national funds through the FCT/MCTES (PIDDAC), FCT/MECI: LEPABE, UID/00511/2025 (https://doi.org/10.54499/UID/00511/2025), UID/PRR/00511/2025 (https://doi.org/10.54499/UID/PRR/00511/2025) and ALiCE, LA/P/0045/2020 (https://doi.org/10.54499/LA/P/0045/2020).

Data Availability Statement: The original contributions presented in this study are included in the article/Supplementary Material. Further inquiries can be directed to the corresponding author.

Conflicts of Interest: The authors declare no conflict of interest.

References

1. Baldé, C.P.; D'Angelo, E.; Luda, V.; Deubzer, O.; Kuehr, R. *Global Transboundary E-Waste Flows Monitor*; United Nations Institute for Training and Research (UNITAR): Bonn, Germany, 2022.
2. Ly, N.H.; Joo, S.W.; Choo, J.; Vasseghian, Y.; Cho, J.; Rezania, S. Sustainable Cutting-Edge Techniques for Gold Valorization from Electronic Wastes. *Chem. Eng. J.* **2023**, *471*, 144324. [CrossRef]
3. Mao, S.; Kang, Y.; Zhang, Y.; Xiao, X.; Zhu, H. Fractional Grey Model Based on Non-Singular Exponential Kernel and Its Application in the Prediction of Electronic Waste Precious Metal Content. *ISA Trans.* **2020**, *107*, 12–26. [CrossRef] [PubMed]
4. Niu, B.; Shanshan, E.; Xu, Z.; Guo, J. How to Efficient and High-Value Recycling of Electronic Components Mounted on Waste Printed Circuit Boards: Recent Progress, Challenge, and Future Perspectives. *J. Clean. Prod.* **2023**, *415*, 1377815. [CrossRef]
5. Li, K.; Zhang, L.; Xu, Z. Decomposition Behaviour and Mechanism of Epoxy Resin from Waste Integrated Circuits Under Supercritical Water Condition. *J. Hazard. Mater.* **2019**, *374*, 356–364. [CrossRef] [PubMed]
6. Lee, C.H.; Tang, L.W.; Popuri, S.R. A Study on the Recycling of Scrap Integrated Circuits by Leaching. *Waste Manag. Res.* **2011**, *29*, 677–685. [CrossRef] [PubMed]
7. Debnath, B.; Roychowdhury, P.; Kundu, R. Electronic Components (EC) Reuse and Recycling—A New Approach Towards WEEE Management. *Procedia Environ. Sci.* **2016**, *35*, 656–668. [CrossRef]
8. Ismail, H.; Hanafiah, M.M. An Overview of LCA Application in WEEE Management: Current Practices, Progress and Challenges. *J. Clean. Prod.* **2019**, *5*, 79–93. [CrossRef]
9. Liu, Y.; Li, K.; Guo, J.; Xu, Z. Impact of the Operating Conditions on the Derived Products and the Reaction Mechanism in Vacuum Pyrolysis Treatment of the Organic Material in Waste Integrated Circuits. *J. Clean. Prod.* **2018**, *197*, 1488–1497. [CrossRef]
10. Wang, X.; Huang, W.; Yan, B.; Zhou, S.; Zhu, X.; Wang, Z.; Cheng, Z.; Chen, G. E-Waste Recycling: Integrated Life Cycle Assessment and Techno-Economic Analysis Unravels Pyrometallurgy's Edge and Delivers an Optimization Framework for Recovering Waste Printed Circuit Boards. *Waste Manag.* **2025**, *207*, 115135. [CrossRef] [PubMed]
11. Panda, R.; Dinkar, O.S.; Kumari, A.; Gupta, R.; Jha, M.K.; Pathak, D.D. Hydrometallurgical Processing of Waste Integrated Circuits (ICs) to Recover Ag and Generate Mix Concentrate of Au, Pd and Pt. *J. Ind. Eng. Chem.* **2021**, *93*, 315–321. [CrossRef]
12. Birloaga, I.; Vegliò, F. Study of Multi-Step Hydrometallurgical Methods to Extract the Valuable Content of Gold, Silver and Copper from Waste Printed Circuit Boards. *J. Environ. Chem. Eng.* **2016**, *4*, 20–29. [CrossRef]
13. Sethurajan, M.; van Hullebusch, E.D.; Fontana, D.; Akcil, A.; Deveci, H.; Batinic, B.; Leal, J.P.; Gasche, T.A.; Kucuker, M.A.; Kuchta, K.; et al. Recent Advances on Hydrometallurgical Recovery of Critical and Precious Elements from End of Life Electronic Wastes—A Review. *Crit. Rev. Environ. Sci. Technol.* **2019**, *49*, 212–275. [CrossRef]
14. Wang, H.; Zhang, S.; Li, B.; Pan, D.; Wu, Y.; Zuo, T. Recovery of Waste Printed Circuit Boards Through Pyrometallurgical Processing: A Review. *Resour. Conserv. Recycl.* **2017**, *8*, 209–218. [CrossRef]
15. Panda, R.; Dinkar, O.S.; Jha, M.K.; Pathak, D.D. Recycling of Gold from Waste Electronic Components of Devices. *Korean J. Chem. Eng.* **2020**, *37*, 111–119. [CrossRef]
16. Gómez, M.; Grimes, S.; Fowler, G. Development of Complete Hydrometallurgical Processes for Gold Recovery from ICs and CPUs Using Ionic Liquids. *J. Environ. Manag.* **2024**, *362*, 121306. [CrossRef] [PubMed]
17. Binnemans, K.; Jones, P.T. Ionic Liquids and Deep-Eutectic Solvents in Extractive Metallurgy: Mismatch Between Academic Research and Industrial Applicability. *J. Sustain. Metall.* **2023**, *9*, 423–438. [CrossRef]

18. Aylmore, M.G. Alternative Lixiviants to Cyanide for Leaching Gold Ores. In *Gold Ore Processing: Project Development and Operations*; Elsevier: Amsterdam, The Netherlands, 2016; pp. 447–484. [CrossRef]
19. Rigoldi, A.; Trogu, E.F.; Marcheselli, G.C.; Artizzu, F.; Picone, N.; Colledani, M.; Deplano, P.; Serpe, A. Advances in Recovering Noble Metals from Waste Printed Circuit Boards (WPCBs). *ACS Sustain. Chem. Eng.* **2019**, *7*, 1308–1317. [CrossRef]
20. Bożejewicz, D.; Witt, K.; Kaczorowska, M.A.; Urbaniak, W.; Ośmiałowski, B. The Application of 2,6-Bis(4-Methoxybenzoyl)-Diaminopyridine in Solvent Extraction and Polymer Membrane Separation for the Recovery of Au(III), Ag(I), Pd(II) and Pt(II) Ions from Aqueous Solutions. *Int. J. Mol. Sci.* **2021**, *22*, 179123. [CrossRef] [PubMed]
21. Tomizaki, K.Y.; Okamoto, T.; Tonoda, T.; Imai, T.; Asano, M. Selective Gold Recovery from Homogenous Aqueous Solutions Containing Gold and Platinum Ions by Aromatic Amino Acid-Containing Peptides. *Int. J. Mol. Sci.* **2020**, *21*, 5060. [CrossRef] [PubMed]
22. Doidge, E.D.; Kinsman, L.M.M.; Ji, Y.; Carson, I.; Duffy, A.J.; Kordas, I.A.; Shao, E.; Tasker, P.A.; Ngwenya, B.T.; Morrison, C.A.; et al. Evaluation of Simple Amides in the Selective Recovery of Gold from Secondary Sources by Solvent Extraction. *ACS Sustain. Chem. Eng.* **2019**, *7*, 15019–15029. [CrossRef]
23. Sadeghi, S.M.; Soares, H.M.V.M. A Sustainable Hydrometallurgical Strategy for Recycling Efficiently Platinum from Spent Reforming Petroleum Catalyst. *Environ. Sci. Pollut. Res.* **2023**, *30*, 101410–101423. [CrossRef] [PubMed]
24. Wołowicz, A.; Hubicki, Z. Adsorption Characteristics of Noble Metals on the Strongly Basic Anion Exchanger Purolite A-400TL. *J. Mater. Sci.* **2014**, *49*, 6191–6202. [CrossRef]
25. Fritz, B.; Aichele, C.; Schmidt, M. Environmental Impact of High-Value Gold Scrap Recycling. *Int. J. Life Cycle Assess.* **2020**, *25*, 1930–1941. [CrossRef] [PubMed]
26. Oke, E.A.; Potgieter, H. Discarded E-Waste/Printed Circuit Boards: A Review of Their Recent Methods of Disassembly, Sorting and Environmental Implications. *J. Mater. Cycles Waste Manag.* **2024**, *81*, 1277–1293. [CrossRef]
27. Iannicelli-Zubiani, E.M.; Giani, M.I.; Recanati, F.; Dotelli, G.; Puricelli, S.; Cristiani, C. Environmental Impacts of a Hydrometallurgical Process for Electronic Waste Treatment: A Life Cycle Assessment Case Study. *J. Clean. Prod.* **2017**, *140*, 1204–1216. [CrossRef]
28. Francini, A.; Cornelio, A.; Bontempi, E.; Serpe, A.; Ferrari, A.M.; Neri, P.; Rosa, R. Environmental Assessment of Noble Metals Recovery from E-Waste: An ESCAPE and LCA-Based Comparative Analysis towards Design for Sustainability. *J. Clean. Prod.* **2025**, *534*, 147016. [CrossRef]
29. Bachér, J.; Rintala, L.; Horttanainen, M. The Effect of Crusher Type on Printed Circuit Board Assemblies' Liberation and Dust Generation from Waste Mobile Phones. *Miner. Eng.* **2022**, *185*, 107674. [CrossRef]
30. Duan, C.; Zhao, Y.; He, J.; Zhou, N. Research on Liberation Mechanism of the Impact Crushing Waste Printed Circuit Board. *Adv. Mater. Res.* **2010**, *113–116*, 730–734. [CrossRef]
31. Marra, A.; Cesaro, A.; Belgiorno, V. Separation Efficiency of Valuable and Critical Metals in WEEE Mechanical Treatments. *J. Clean. Prod.* **2018**, *186*, 490–498. [CrossRef]
32. Barnwal, A.; Dhawan, N. Physical Processing of Discarded Integrated Circuits for Recovery of Metallic Values. *JOM* **2020**, *72*, 2730–2738. [CrossRef]
33. Barnwal, A.; Dhawan, N. Recovery of Metals from Discarded Integrated Circuits. *Min. Metall. Explor.* **2020**, *20*, 1641–1651. [CrossRef]
34. Ajiboye, E.A.; Olasehinde, E.F.; Adebayo, A.O.; Ajayi, O.O.; Ghosh, M.K.; Basu, S. Extraction of Cu, Zn, and Ni from Waste Silica-Rich Integrated Circuits by Sulfation Roasting and Water Leaching. *Chem. Pap.* **2020**, *74*, 663–671. [CrossRef]
35. Sousa, R.; Regufe, M.J.; Fiúza, A.; Leite, M.M.; Futuro, A. A Systematic Review of Sustainable Gold Extraction from Raw Ores Using Alternative Leaching Reagents. *Extr. Ind. Soc.* **2022**, *21*, 101018. [CrossRef]
36. Al Adday, F.; Awad, A.; Aleghnimat, R.; Bassam, H.; Khater, A. Fresh and Hardened Properties of Recycled Concrete Aggregate Modified by Iron Powder and Silica. *Int. J. GEOMATE* **2019**, *16*, 222–230. [CrossRef]
37. Chandrashekhar, V.G.; Senthamarai, T.; Kadam, R.G.; Malina, O.; Kašlík, J.; Zbořil, R.; Gawande, M.B.; Jagadeesh, R.V.; Beller, M. Silica-Supported Fe/Fe–O Nanoparticles for the Catalytic Hydrogenation of Nitriles to Amines in the Presence of Aluminium Additives. *Nat. Catal.* **2022**, *5*, 20–29. [CrossRef]
38. Suo, H.; Wang, S.; Zhang, C.; Xu, J.; Wu, B.; Yang, Y.; Xiang, H.; Li, Y.W. Chemical and Structural Effects of Silica in Iron-Based Fischer-Tropsch Synthesis Catalysts. *J. Catal.* **2012**, *286*, 111–123. [CrossRef]
39. Wielers, A.F.H.; Kock, A.J.H.M.; Hop, C.E.C.A.; Geus, J.W.; van der Kraan, A.M. The reduction behavior of silica-supported and alumina-supported iron catalysts: A Mössbauer and infrared spectroscopic study. *J. Catal.* **1989**, *117*, 1–18. [CrossRef]
40. Finkelstein, N.P.; Hancock, R.D. A New Approach to the Chemistry of Gold. *Gold Bull.* **1974**, *7*, 72–77. [CrossRef]
41. Nicol, M.J.; Fleming, C.A.; Paul, R.L. *The Chemistry of the Extraction of Gold*; South African Institute of Mining and Metallurgy: Johannesburg, South Africa, 1987.
42. Jeffrey, M.I.; Breuer, P.L.; Choo, W.L. A Kinetic Study That Compares the Leaching of Gold in the Cyanide, Thiosulfate, and Chloride Systems. *Metall. Mater. Trans. B* **2001**, *32B*, 979–986. [CrossRef]

43. Baghalha, M. Leaching of an Oxide Gold Ore with Chloride/Hypochlorite Solutions. *Int. J. Miner. Process.* **2007**, *82*, 178–186. [CrossRef]
44. He, Y.; Xu, Z. Recycling Gold and Copper from Waste Printed Circuit Boards Using Chlorination Process. *RSC Adv.* **2015**, *5*, 8957–8964. [CrossRef]
45. Neto, I.F.F.; Soares, H.M.V.M. Simple and Near-Zero-Waste Processing for Recycling Gold at a High Purity Level from Waste Printed Circuit Boards. *Waste Manag.* **2021**, *135*, 90–97. [CrossRef] [PubMed]
46. Machesky, M.L.; Rose, A.W. Adsorption of Gold(III~chloride and Gold(I)-Thiosulfate Anions by Goethite. *Geochim. Cosmochim. Acta* **1991**, *55*, 769–776. [CrossRef]
47. Hasab, M.G.; Rashchi, F.; Raygan, S. Chloride-Hypochlorite Leaching and Hydrochloric Acid Washing in Multi-Stages for Extraction of Gold from a Refractory Concentrate. *Hydrometallurgy* **2014**, *142*, 56–59. [CrossRef]
48. Spiegel, M.; Zahs, A.; Grabke, H.J. Fundamental Aspects of Chlorine Induced Corrosion in Power Plants. *Mater. High Temp.* **2003**, *20*, 153–159. [CrossRef]
49. DeCoste, J.B.; Browe, M.A.; Wagner, G.W.; Rossin, J.A.; Peterson, G.W. Removal of Chlorine Gas by an Amine Functionalized Metal-Organic Framework via Electrophilic Aromatic Substitution. *Chem. Commun.* **2015**, *51*, 12474–12477. [CrossRef] [PubMed]
50. Jeon, S.; Tabelin, C.B.; Takahashi, H.; Park, I.; Ito, M.; Hiroyoshi, N. Interference of Coexisting Copper and Aluminum on the Ammonium Thiosulfate Leaching of Gold from Printed Circuit Boards of Waste Mobile Phones. *Waste Manag.* **2018**, *81*, 148–156. [CrossRef] [PubMed]
51. Bui, T.H.; Jeon, S.; Lee, Y. Facile Recovery of Gold from E-Waste by Integrating Chlorate Leaching and Selective Adsorption Using Chitosan-Based Bioadsorbent. *J. Environ. Chem. Eng.* **2021**, *9*, 104661. [CrossRef]
52. Olteanu, A.F.; Dobre, T.; Panturu, E.; Radu, A.D.; Akcil, A. Experimental Process Analysis and Mathematical Modeling for Selective Gold Leaching from Slag Through Wet Chlorination. *Hydrometallurgy* **2014**, *144–145*, 170–185. [CrossRef]
53. Fu, L.; Zhang, L.; Wang, S.; Cui, W.; Peng, J. Synergistic Extraction of Gold from the Refractory Gold Ore via Ultrasound and Chlorination-Oxidation. *Ultrason. Sonochem.* **2017**, *37*, 471–477. [CrossRef] [PubMed]
54. Filcenco-Olteanu, A.; Dobre, T.; Rădulescu, R.; Panţuru, E.; Panţuru, R. Selective Recovery of Gold from Hydrochloric Solutions with Amberlite XAD-7 Ion-Exchange Resin. *UPB Sci. Bull. Ser. B Chem. Mater. Sci.* **2010**, *72*, 233–242.
55. van Deventer, J.; Bazhko, V.; Yahorava, V. *Premier Products Gold Selective Ion Exchange Resin vs. Activated Carbon for Recovery of Gold Comparison of Gold-Selective Ion Exchange Resins and Activated Carbon for the Recovery of Gold from Copper-Gold Leach Liquors Gols Selected*; ALTA Metallurgical Services: Perth, Australia, 2000.
56. Azizitorghabeh, A.; Mahandra, H.; Ramsay, J.; Ghahreman, A. Selective Gold Recovery from Pregnant Thiocyanate Leach Solution Using Ion Exchange Resins. *Hydrometallurgy* **2023**, *218*, 106055. [CrossRef]
57. European Union. Directive (EU) 2024/3019 on Urban Wastewater Treatment. In *Official Journal of the European Union*; European Union: Luxembourg, 2024.
58. Tian, Y.; Olivetti, E.A. Strategies for Industrial Residue Valorization Through Metal Recovery, Use in Construction, or CO_2 Mineralization. *Waste Manag.* **2025**, *203*, 114824. [CrossRef] [PubMed]
59. Shields, V.R.; Robshaw, T.J.; Porter, C.P.; Amphlett, J.T.M.; Hides, A.; Bruce, R.; Cordiner, J.; Ogden, M.D. Gold Recovery from Synthetic Mine Tailings Leachate Using Chelating Ion Exchange Resins with Thiosulfate-Thiourea Lixiviant. *Resour. Conserv. Recycl. Adv.* **2023**, *19*, 200182. [CrossRef]
60. Alguacil, F.J.; Adeva, P.; Alonso, M. Processing of Residual Gold (III) Solutions via Ion Exchange. *Gold Bull.* **2005**, *38*, 9–13. [CrossRef]
61. Marinho, R.S.; da Silva, C.N.; Afonso, J.C.; da Cunha, J.W.S.D. Recovery of Platinum, Tin and Indium from Spent Catalysts in Chloride Medium Using Strong Basic Anion Exchange Resins. *J. Hazard. Mater.* **2011**, *192*, 1155–1160. [CrossRef] [PubMed]
62. Sadeghi, S. Selective Recycling of Metals from Secondary Resources. Ph.D. Thesis, University of Porto, Porto, Portugal, 2020. [CrossRef]
63. Craw, D.; McLachlan, C.; Negrini, M.; Becker, N. Quantification and Prediction of Bulk Gold Fineness at Placer Gold Mines: A New Zealand Example. *Minerals* **2017**, *7*, 110226. [CrossRef]
64. International Energy Agency. Available online: https://www.iea.org/ (accessed on 24 April 2026).